CHAPTER 27

AN ADDITIONAL PARAMETER FOR THE ZERO CROSSING WAVE DEFINITION AND ITS PROBABILITY DISTRIBUTION

by A. Kimura[1] and T. Ohta[2]

ABSTRACT

In this paper, the distance from the mid point between a wave trough and a consecutive wave crest of a zero-crossing wave (a position of wave height bisection) to the still water level is proposed to be an important zero-crossing wave property. Its roles on certain physical properties of the zero-crossing waves are shown through experimental data in the first part of the paper. Its probability distribution is introduced, in the second part, from the combined probability distribution of the amplitudes of consecutive wave trough and crest of irregular waves. In the last part, the theoretical probability distribution for this property is verified with numerically simulated data for many types of wave spectra.

1. INTRODUCTION

The zero-crossing method has been used to split the irregular wave profile into zero-crossing waves. The overall physical property of irregular waves is evaluated by connecting the relevant physical properties of individual waves and the probability of wave heights and periods. For example, the probability distribution of random wave forces (Kimura et al., 1983) is given as

$$p(f)\,df = \int_S p(H,T)\;dHdT \tag{1}$$

p(H,T) is the combined distribution of wave height H and period T. S is the region in which

$$f \le g(H,T) \le f + df \tag{2}$$

where g(H,T) gives the wave force f of a periodic wave for the wave with H and T.

1 Prof., Dept. of Social Systems Eng., Faculty of Eng., Tottori Univ., 4-101 Koyama Minami, Tottori, Japan

2 Research Associate, Dept. of Social Systems Eng., Faculty of Eng., Tottori Univ., 4-101 Koyama Minami, Tottori, Japan

The physical properties of the zero-crossing wave are approximated usually by those of a periodic wave with the same wave height and period. The draw back of this method ,some times, is that the two properties H and T are not sufficient to express the overall physical wave properties, since the measured and calculated probabilities have shown apparent differences in some physical properties. Therefore some studies have tried to apply supplemental wave properties such as slope of the fore-side face of waves in the examination of wave breaking (Holthuijsen and Herbers, 1986, for example). Among these, important parameters which may affect the physical properties of the zero-crossing wave are listed by the PIANC working group (list of sea state parameters; 1987).
The parameter proposed in this study is not involved in the list but may exert an important effect on the waves in a shallow water region. That is a position of wave height bisection (mean position between the wave crest and trough of a zero-crossing wave).
Two waves in Fig.1 have the same wave height and period but different crest heights. In the ordinary definition, these two waves are recognized as having the same property. Figure 2(a) shows the wave height at the breaking point on 1/20 slope (Seyama et al., 1988). H, L_0 and h are the wave height, deep water wave length and still water depth. Subscript b shows the value measured at the breaking points. The same data (H/H_b) are plotted against h* in Fig.2(b) instead of h , in which h* is the distance from the bottom to the center between wave crest and trough (Fig.1). The scattering of data in Fig.2(a) reduces very much in this figure, therefore, h* works more effectively as a water depth than h. This h* is given by the sum of the still water depth h and the distance d from the still water level to the position of wave height bisection (PWHB; Fig.1). In the next section, the probability distribution for d is introduced theoretically and the result is verified through numerically simulated irregular waves.

2. The definition of d and its characteristics

2.1 Definition

The distance d from the mean water level to PWHB is given by

$$d = (\eta_1 - \eta_2) / 2 \qquad (3)$$

in which η_1 and η_2 are the amplitudes of the wave trough and the consecutive wave crest, respectively. From a definition of the zero-crossing wave, we got $-H/2 < d < H/2$.

2.2 Characteristics of d

The numerically simulated values of d are shown first. The FFT method is used to calculate irregular wave profiles for the Wallops type wave spectrum which is given by

$$S(f) = (f/f_p)^{-m} \exp\left[m/4 \left\{ 1-(f/f_p)^{-4} \right\} \right] \qquad (4)$$

where f_p is 1.0Hz and the interval of the calculated wave profile, Δt is 0.05s. in the numerical simulations. The 7 different values for the shape parameter m (4, 5, 6, 8, 10, 15, 20) in eq.(4) are used in the calculations. The zero-down-cross method is applied in the irregular wave definition. d is calculated applying eq.(3) for each wave. Figures 3 (a), (b) and (c) show the calculated relations between d/H and H/H_m (H_m is the mean wave height) for three values of m (5, 10, 20) in this order. While the spectrum is wide (m=5) d/H distributes up to its limit (-H/2, H/2) where H/H_m

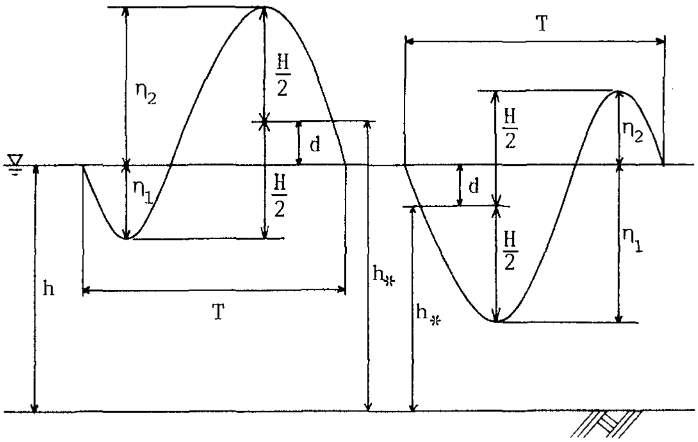

Fig. 1 Zero down cross waves with common H and T

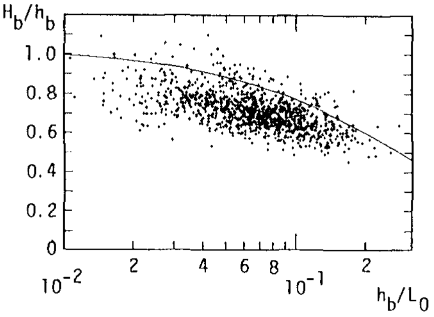

Fig. 2(a) Breaking limit

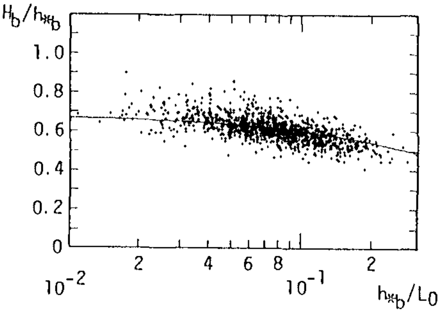

Fig. 2(b) Breaking limit
(modefied water depth)

<1.0. However the fluctuation decreases at the larger values of H/H_m. When m is large ((b),(c)) the fluctuation decreases except for the very small wave height region. From these, the larger the wave height or the narrower the wave spectrum, the more zero-down-cross waves tend to have symmetric profiles.

3. The probability distribution of d

3.1 Two-dimensional Rayleigh distribution

As shown in eq.(3), d is half the difference between η_1 and η_2. If these two values are independent (no correlation), the probability distribution for d is easily given as

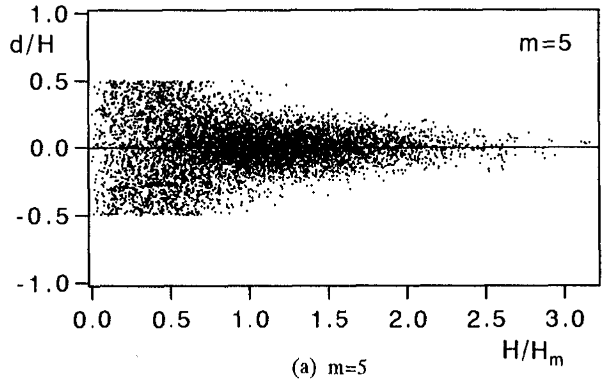

(a) m=5

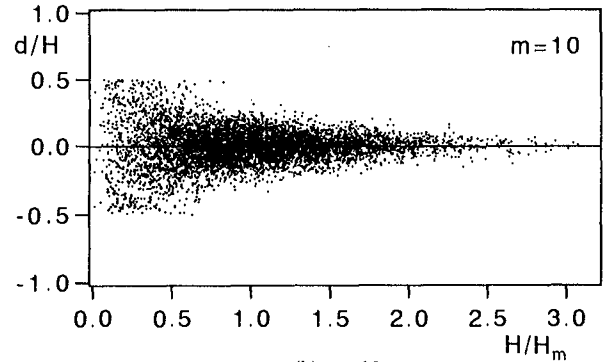

(b) m=10

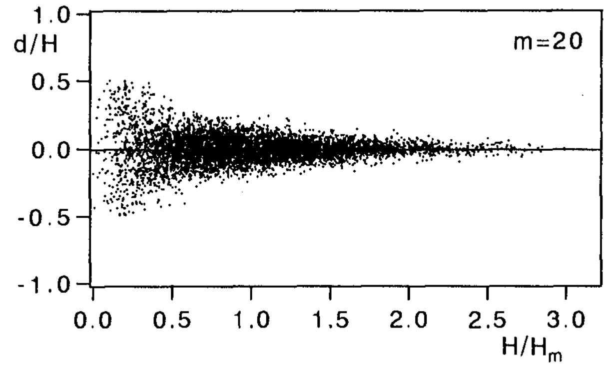

(c) m=20

Fig. 3 Distribution of d/H

$$p(d) = \int p\left(\frac{h_1}{2} + d\right) p\left(\frac{h_1}{2}\right) dh_1 \tag{5}$$

where p(.) is the probability distribution. The time interval between consecutive wave trough and crest is about half the mean wave period on the average. Two values on the wave profile with such a distance inevitably have a correlation. Therefore, this correlation property has to be taken into account when the probability distribution for d is considered. However the theoretical probability distribution of η_i (i=1,2) has not yet been determined. The amplitude of the envelope for the wave profile at the same position of η_i has been used instead (Tayfun et al., 1989) with an error of order ν in the noise theory, where ν is given by

$$\nu = \left(m_0 m_2 / m_1^2 - 1\right)^2 \tag{6}$$

and

$$m_n = \int_0^{\infty} f^n \, S(f) \, df \tag{7}$$

in which S(f) is the power spectrum of waves.

The present study also used the above approximation. Since the theoretical probability distribution for envelopes is the Rayleigh distribution (Rice,1945), the combined distribution for η_1 and η_2 is given by the 2-dimensional Rayleigh distribution (no non-linearlity of the wave is considered in the present study). Expressing the amplitudes of wave envelopes at the position of η_1 and η_2 as A_1 and A_2 respectively, Eq.(3) is approximately expressed as,

$$d = \left(A_1 - A_2\right) / 2 \tag{8}$$

The probability distribution for the normalized amplitude $\xi_i = A_i / A_m$ (i=1,2), where A_m is a mean amplitude, is the Rayleigh distribution.

$$p\left(\xi_i\right) = \frac{\pi}{2} \xi_i \exp\left[-\frac{\pi \xi_i^2}{4} \right] \tag{9}$$

The combined probability distribution of the numerically simulated ξ_1 and ξ_2 agrees well with the 2-dimensional Rayleigh distribution,

$$p\left(\xi_1, \xi_2\right) = \frac{\pi^2 \xi_1 \xi_2}{4\left(1 - \kappa^2\right)} \exp\left[-\frac{\pi^2\left(\xi_1^2 + \xi_2^2\right)}{4\left(1 - \kappa^2\right)} \right] I_0 \left[\frac{\pi \kappa \xi_1 \xi_2}{2\left(1 - \kappa^2\right)} \right] \tag{10}$$

in which I_0 is the 0-th order modified Bessel function of the first kind, and κ is the correlation parameter which is calculated as follows,

$$\kappa = \sqrt{\left(\rho^2 + \lambda^2\right)} / m_0 \tag{11}$$

where

$$\rho = \int_0^{\infty} S(f) \cos 2\pi(f - \overline{f}) \frac{t}{2}\, df$$

$$\lambda = \int_0^{\infty} S(f) \sin 2\pi(f - \overline{f}) \frac{t}{2}\, df$$

$$\overline{f} = m_1 / m_0 \qquad (12)$$

t/2 is the time interval between A_1 and A_2. $T_m/2$ is used for this interval in this study where T_m is the mean wave period. This parameter is explained briefly in 3.3.

Figure 4 shows the comparison between numerically simulated combined frequency distributions of ξ_1 and ξ_2 and eq.(10) (solid line). The values for m in eq.(4) is (a) 5, (b) 10, and (c) 20 respectively. When m=5 the spectrum is that for a fully developed sea condition. Excellent agreements are obtained for all cases.

3.2 The probability distribution of d

Since A_1 and A_2 are amplitudes of the envelope at the consecutive wave trough ξ_1 and crest ξ_2, the wave height is given approximately as,

$$H = A_1 + A_2 \qquad (13)$$

Both sides of eq.(13) are divided by H_m (=$2A_m$, A_m; mean amplitude of the envelope) to normalize,

$$\zeta = (\xi_1 + \xi_2) / 2 \qquad (14)$$

in which $\xi_i/2 = A_i/H_m\,(i=1,2)$ and $\zeta = H/H_m$

From eq.(14),

$$\xi_2 = 2\zeta - \xi_1 \qquad (15)$$

Substituting eq.(15) into eq.(10), the combined distribution of ξ_1 and ζ is obtained.

$$p(\xi_1, \zeta) = \frac{\pi^2 \xi_1 (2\zeta - \xi_1)}{2(1 - \kappa^2)} \exp\left[-\frac{\pi^2 \left\{ \xi_1^2 + (2\xi - \xi_1)^2 \right\}}{4(1 - \kappa^2)} \right] I_0\left[\frac{\pi \kappa \xi_1 (2\zeta - \xi_1)}{2(1 - \kappa^2)} \right] \qquad (16)$$

Integration of eq.(16) brings the probability distribution for ζ

$$p(\zeta) = \int_0^{2\zeta} p(\xi_1, \zeta)\, d\xi_1 \qquad (17)$$

Since the analytical expression of this integration is difficult, a numerical calculation is used. The region of the integration is given from the definition of ξ_1, $\xi_2 > 0$. To normalize the region,

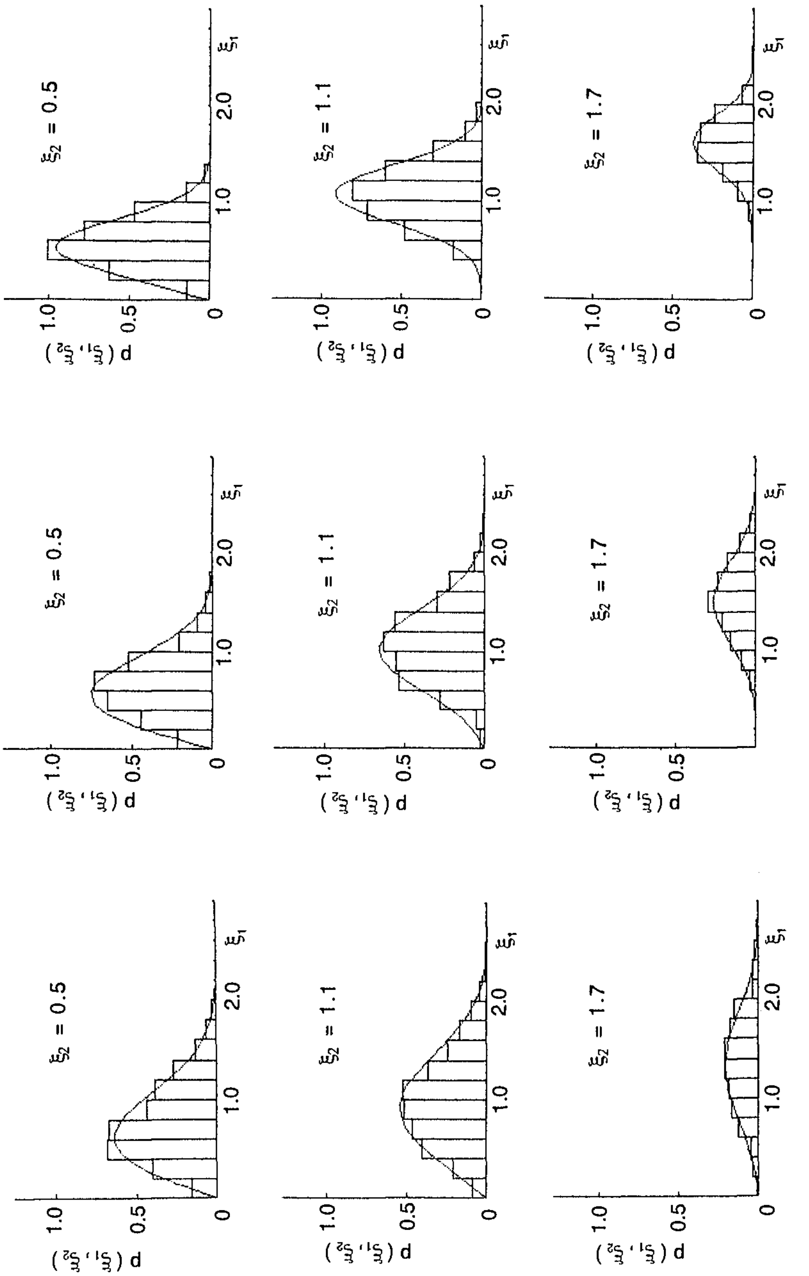

(a) m=5 (b) m=10 (c) m=20

Fig. 4 Combined probability distribution of ξ_1 and ξ_2

eq.(8) is divided by H_m.

$$\delta = (\xi_1 - \xi_2) / 4 \tag{18}$$

Substitution of eq.(15) into eq.(18) brings

$$\delta = (\xi_1 - \zeta) / 2 \tag{19}$$

then

$$\xi_1 = 2\delta + \zeta \tag{20}$$

Substituting this relation in eq.(16), the combined distribution of δ and ζ is obtained.

$$p(\delta, \zeta) = \frac{\pi^2 (\zeta^2 - 4\delta^2)}{1 - \kappa^2} \exp\left[-\frac{\pi (\zeta^2 + 4\delta^2)}{2(1-\kappa^2)}\right] I_0\left[\frac{\pi \kappa (\zeta^2 - 4\delta^2)}{2(1-\kappa^2)}\right] \tag{21}$$

From the definition,

$$-H/2 < d < H/2 \tag{22}$$

we obtain

$$-\zeta/2 < d < \zeta/2 \tag{23}$$

Since δ in eq.(21) changes the range following the change of ζ, the new parameter which is given in the next equation is introduced.

$$\varepsilon = \delta / \zeta \ (=d/H) \tag{24}$$

ε takes the value only from -1/2 to 1/2 regardless of ζ. Substitution of this parameter in eq.(21) we obtain,

$$p(\varepsilon, \zeta) = \frac{\pi^2 \zeta^3 (1 - 4\varepsilon^2)}{1 - \kappa^2} \exp\left[-\frac{\pi \zeta^2 (\zeta + 4\varepsilon^2)}{2(1-\kappa^2)}\right] I_0\left[\frac{\pi \kappa \zeta^2 (1 - 4\varepsilon^2)}{2(1-\kappa^2)}\right] \tag{25}$$

The conditional distribution of ε for given ζ, is calculated as

$$p(\varepsilon \mid \zeta) = p(\varepsilon, \zeta) / p(\zeta) \tag{26}$$

3.3 Time interval between A_1 and A_2

κ which is calculated by eq.(11) plays a very important role in this theory. The representative frequency $\bar{f}$ is usually given by eq.(12) and the time interval t/2 between A_1 and A_2 is approximately given by the mean wave period. Two definitions for the mean wave period have been used. They are

$$T_{01} = m_0 / m_1$$
$$T_{02} = \sqrt{m_0 / m_2} \tag{27}$$

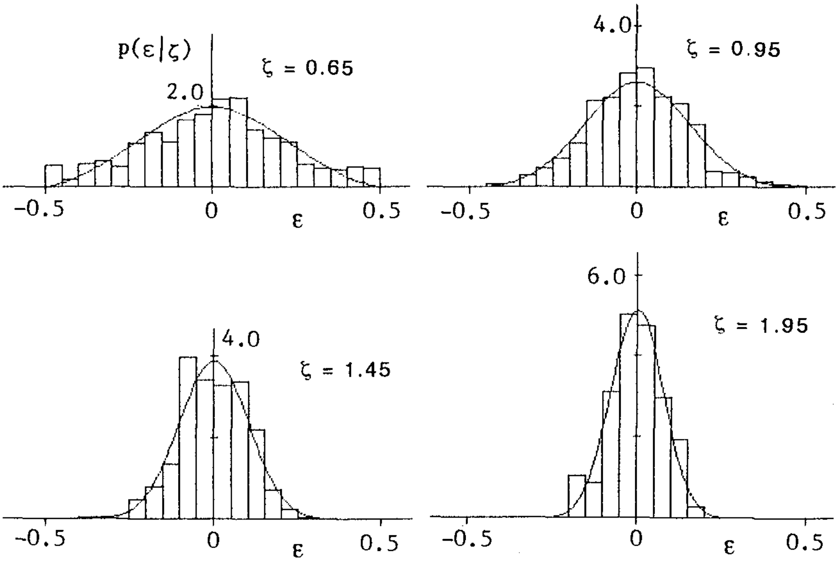

Fig. 5(a) Conditional probability distribution for ε (m=5)

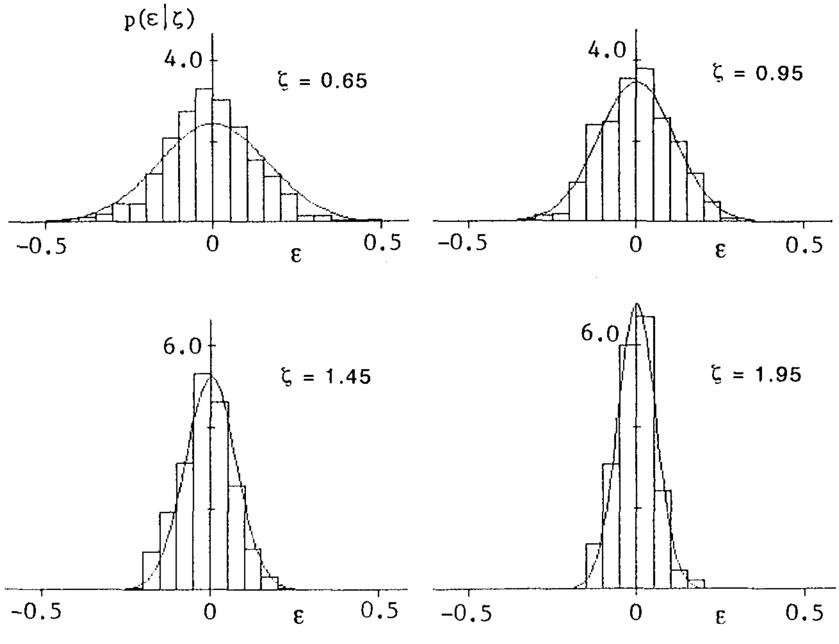

Fig. 5(b) Conditional probability distribution for ε (m=10)

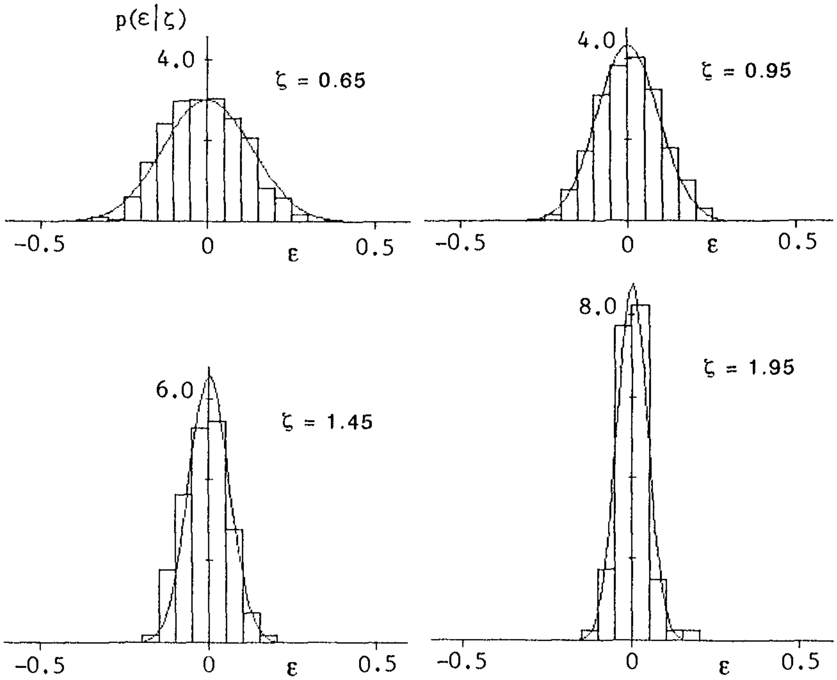

Fig. 5(c) Conditional probability distribution for ε (m=20)

The numerical calculations with different values of m in eq.(4) show that T_{02} is always closer to the calculated mean zero-crossing wave period than T_{01}. Therefore T_{02} is used for T_m in this study.

4. Verification of the theoretical distribution

Figure 5 shows the comparison between $p(\varepsilon \mid \zeta)$ and the numerically simulated values of ε for the several different wave spectra (a) m=5, (b) m=10, (c) m=20. The solid curves shows the theoretical distributions and the columns are the frequency distributions of the numerically simulated data of ε. Calculated values of ε which fall in the shown intervals of ζ are sorted into ranks of width $\Delta\varepsilon$=0.05 from ε=-0.5 to 0.5. The agreement between the theory and the simulated data are good in all cases except for the very small part of ζ. This discrepancy in the region of small ζ may be induced by the value of κ used in the calculation of eq.(12), since the time interval between the consecutive wave trough and crest for a small wave is smaller than the average value. However when ζ is larger than 0.6~0.7, the theoretical distributions always show good agreements with the data. Fig. 6 shows the comparison between the theoretical standard deviation (solid line) for ε which is given by

$$\sigma = \left\{ \overline{\varepsilon^2} - (\overline{\varepsilon})^2 \right\}^{1/2} \tag{28}$$

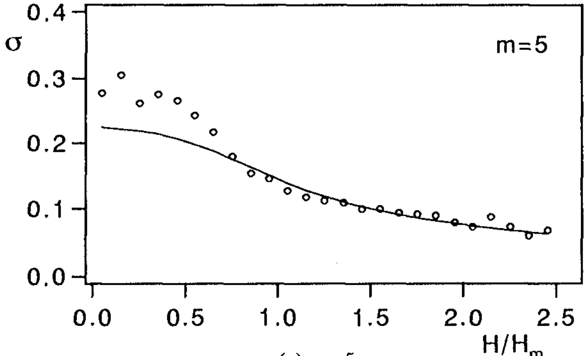

(a) m=5

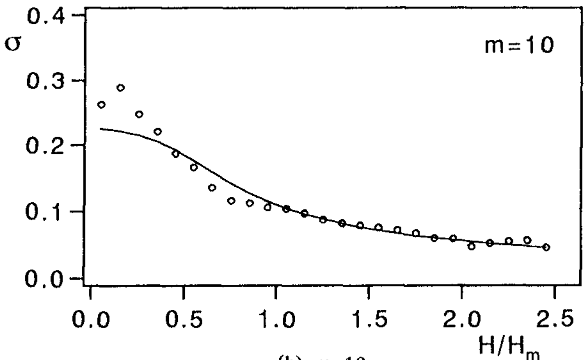

(b) m=10

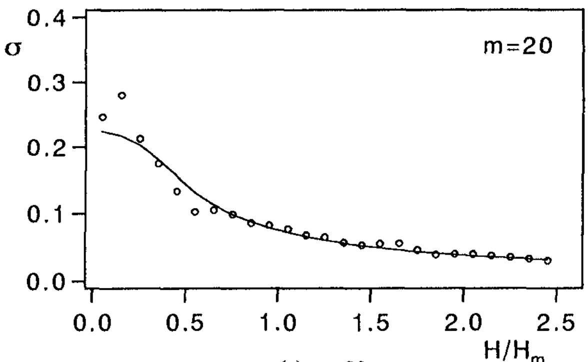

(c) m=20

Fig. 6 Standard deviations of ε

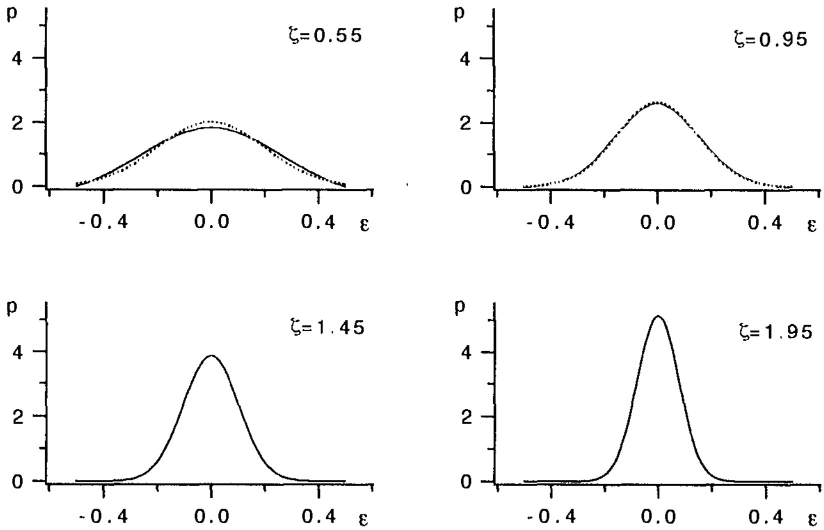

Fig. 7 Comparison between $p(\varepsilon|\zeta)$ and the normal distribution (m=5)
(solid line; $p(\varepsilon|\zeta)$, dotted line; the normal distribution)

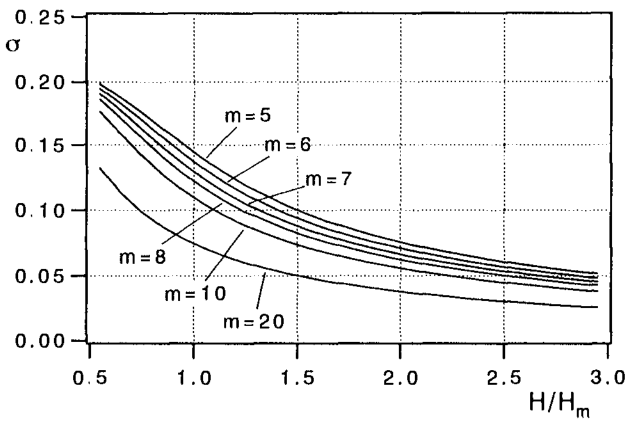

Fig. 8 Theoretical standard deviation for $p(\varepsilon|\zeta)$

where

$$\overline{\varepsilon^2} = \int_{-1/2}^{1/2} \varepsilon^2 \, p(\varepsilon \mid \zeta) \, d\varepsilon$$

$$\bar{\varepsilon} = \int_{-1/2}^{1/2} \varepsilon \, p(\varepsilon \mid \zeta) \, d\varepsilon \tag{29}$$

and the standard deviations of the numerically simulated data (white circle). Except for the smaller part than ζ= 0.6~0.7 their agreements are good. As can be observed in fig. 5, the theoretical distribution $p(\varepsilon \mid \zeta)$ has a very close form to the normal distribution. Fig.7 shows the comparisons between $p(\varepsilon \mid \zeta)$ (solid line) and the normal distribution (dotted line) of the zero mean and the standard deviation calculated from eq.(28). The probability distribution $p(\varepsilon \mid \zeta)$ used in the calculation is that for m=5 (eq.12) in this case. The agreements between $p(\varepsilon \mid \zeta)$ and the normal distribution always agree well regardless of the spectrum width when the calculated value of the standard deviation by eq.(28) is used beside zero mean. Fig.8 shows the theoretical standard deviation for $p(\varepsilon \mid \zeta)$ for the several different spectra (eq.4).

5. Conclusion

Additional property for the zero crossing wave is proposed newly in this study. That is the distance from the mean water level to the mean position between the consecutive wave trough and crest. Its theoretical distribution is introduced and compared with the numerically simulated data. The theoretical distribution shows excellent agreement with the numerically simulated data regardless of the spectrum width. The theoretical distribution has a very close form to the normal distribution and can be approximated with that distribution, if the standard deviation shown in Fig.8 and the zero mean is applied.

References

Holthuijsen, L.H. and T.H.C. Herbers: Statistics of breaking waves observed as white caps in the open sea, Journal of Physical Oceanography, Vol.16, No.2, pp.290-297, 1986.

Kimura, A. and A. Seyama: Statistical properties of displacements of fixed-type offshore structures, Coastal Engineering in Japan, Vol.26, pp.193-207, 1983.

PIANC: List of sea state parameters, Proc. IAHR seminar, Maritime Hydraulics Section, pp.17-44, 1986.

Rice, S. O. : Mathematical analysis of random noise, Selected papers on noise and stochastic process, N. Wax, ed., Dover, New York, N. Y. , pp.133-294, 1954)

Seyama, A. and A. Kimura: The measured properties of irregular wave breaking and wave height change after breaking on the slope, Proc. 21st ICCE, pp.419-432, 1988.

Tayfun, M. A. and J. M. Lo: Envelope, phase, and narrow-band models of sea waves, Journal of Water way, Port, Coastal and Ocean Engineering, ASCE, Vol.115, No. 5, pp.594-613, 1989.